

Columnar Organization of Directionally Selective Cells in Visual Area MT of the Macaque

THOMAS D. ALBRIGHT, ROBERT DESIMONE, AND CHARLES G. GROSS

*Department of Psychology, Princeton University, Princeton, New Jersey 08544; and
Laboratory of Neuropsychology, National Institute of Mental Health,
Bethesda, Maryland 20205*

SUMMARY AND CONCLUSIONS

1. We recorded from single neurons in visual area MT of the macaque in order to examine the spatial distribution of its directionally selective cells. The animals were paralyzed and anesthetized with nitrous oxide.

2. All MT neurons ($n = 614$) responded better to moving stimuli than to stationary stimuli. For 55% of the neurons, responses to moving stimuli were independent of stimulus color, shape, length, or orientation. For the remaining cells, stimulus length affected the response magnitude and tuning bandwidth but not the preferred direction.

3. MT neurons were divided into four categories on the basis of their sensitivity to moving stimuli: 60% responded exclusively to one direction of motion, 24% responded best to one direction with a weaker response in the opposite direction, 8% responded equally well to two opposite directions of motion, and 8% responded equally well to all directions of motion.

4. The direction preferences of successively sampled cells on a penetration either changed by small increments or occasionally by approximately 180° . Thus, there is a systematic representation of direction of motion. The representation of axis of motion, i.e., the orientation of the path along which a stimulus moves, is more continuous than the representation of direction of motion.

5. There was a systematic relationship between penetration angle and rate of change of preferred axis of motion, indicating that cells with a similar axis of motion preference are arranged in vertical columns. Furthermore, axis of motion columns appear to exist in the

form of continuous slabs in area MT. The size of these slabs is such that 180° of axis of motion are represented in 400–500 μm of cortex.

6. There was also a systematic relationship between penetration angle and frequency of 180° reversals, indicating that cells with a similar direction of motion preference are also organized in vertical columns and cells with opposite direction preferences are located in adjacent columns within a single axis of motion column.

7. Just as in macaque striate cortex where approximately 500 μm of cortex contain the mechanism for the local analysis of stimulus orientation, so in MT approximately 500 μm of cortex contain the mechanism for the local analysis of stimulus motion.

INTRODUCTION

The concept of columnar organization has been of fundamental importance in understanding the functions of the cerebral cortex, especially the primary sensory areas. In macaques, the primary visual cortex (V1), striate cortex, contains columns for ocular dominance (14, 20), orientation (15, 17), color (22), and perhaps spatial frequency (26). Beyond striate cortex there is a multiplicity of additional visual areas but relatively little is known about their function or organization (30, 33, 34). Delineating the types of columnar organization in these extrastriate areas may give us insight into the role these areas play in vision.

The most extensively studied of the extrastriate visual areas is area MT. Area MT is a visuotopically organized area located in the caudal third of the posterior bank of the

superior temporal sulcus (STS) (10, 29). MT receives direct projections from both the primary visual cortex and the second visual area (V2) (28, 29) and can be distinguished from the surrounding cortex on the basis of its heavy myelination (10, 28, 29). The most striking physiological property of MT is the large proportion of cells selective for the direction of stimulus motion (21, 29, 31). In an early study of area MT, Zeki (31) reported a tendency for cells with similar direction preferences to be located in clusters, suggesting some type of orderly arrangement of cells with this property. Van Essen et al. (29) and Maunsell and Van Essen (21) in the macaque and Baker et al. (4) in the owl monkey have reported a similar clustering of directionally selective cells in area MT. In the present study we systematically investigated the spatial arrangement of directionally selective cells in area MT. We found a columnar organization for preferred axis of motion and for preferred direction of motion. The organization is similar to that of the orientation column system of striate cortex. These results lend further support to the notion that columns are a basic feature of the functional organization of the cerebral cortex.

METHODS

Animal preparation and maintenance

Four *Macaca fascicularis* weighing between 4 and 5 kg were each recorded from 7–9 times over a 4-wk period. One week prior to the first recording session, a 3-cm-diameter stainless steel cylinder and a head bolt oriented in the stereotaxic planes were affixed to the animal's skull with screws and dental acrylic. The exposed bone inside the cylinder was sealed with a thin layer of acrylic and a stainless steel cap was then placed on the cylinder. Surgical procedures were performed under ketamine (Ketaset) anesthesia, using an initial dose of 35 mg/kg and supplemented with 50 mg as necessary; 2.5 mg of Valium were also used.

On the day of the recording session the animal was given a restraining dose of ketamine (4 mg/kg) and then anesthetized with halothane in a mixture of nitrous oxide and oxygen. The head was held firmly in a stereotaxic apparatus by means of the head bolt and a specially designed holder attached to the apparatus. (This method eliminates the potentially painful pressure of ear and eye bars, gives unobstructed access to the entire visual field, and allows the animal to be placed repeatedly in the stereotaxic apparatus without significant error.)

After the cap was removed from the cylinder a hole was drilled through the acrylic layer and bone and the dura left intact. Halothane anesthesia was then discontinued, and the animal was maintained on a 7:3 mixture of nitrous oxide and oxygen and immobilized with an intravenous infusion of pancuronium bromide (Pavulon) in saline. Paralysis was maintained with an infusion rate of 0.08 mg·kg⁻¹·h⁻¹. Body temperature was maintained at 37–38°C with a heating pad, and the respiratory rate was adjusted to give an end-tidal carbon dioxide level of about 4%. The pupils were dilated with cyclopentolate (Cyclogyl, 1%) and the corneas were covered with contact lenses selected to focus the eyes on the 57-cm-distant rear-projection tangent screen.

Recording sessions generally continued for 12–36 h. One hour before the end of the experiment, the paralytic agent was discontinued. The cylinder was washed out and filled with saline and the animal allowed to recover. Usually within 3 h the animal was alert and active in its home cage. At least 2 days separated successive recording sessions.

Recording

Varnish-coated tungsten microelectrodes with exposed tips of 10 μm or less were used to record extracellular potentials from single isolated cells. Cells in MT were sampled on long microelectrode penetrations ranging from nearly normal to the cortical surface to nearly tangential. In one animal, recordings were confined to the cortex representing an area of the visual field within approximately 10° of the fovea. In the remaining three animals, recordings extended into the cortex representing the lower visual field at eccentricities ranging from approximately 5 to 30°.

In order to make penetrations either normal or tangential to the surface of MT, we used two different angled approaches. For the tangential penetrations, the electrodes were angled down the posterior bank of STS, 40° from vertical in the parasagittal plane (see Fig. 1). These penetrations entered MT at its posterior dorsolateral border after passing through several millimeters of visual cortex posterior to MT. For the normal penetrations, the electrodes were angled 30° from vertical in the opposite direction from the tangential penetrations (see Fig. 1). These penetrations passed through the lateral surface of area 7 and through the anterior bank of STS before reaching area MT.

Single cells were recorded at closely spaced intervals through the cortex. In the majority of penetrations the optimal direction of motion and the approximate range of directions through which a response could be elicited were determined for a single cell every 50 μm along the electrode track. In two penetrations made parallel to the cortical surface the optimal direction and range were de-

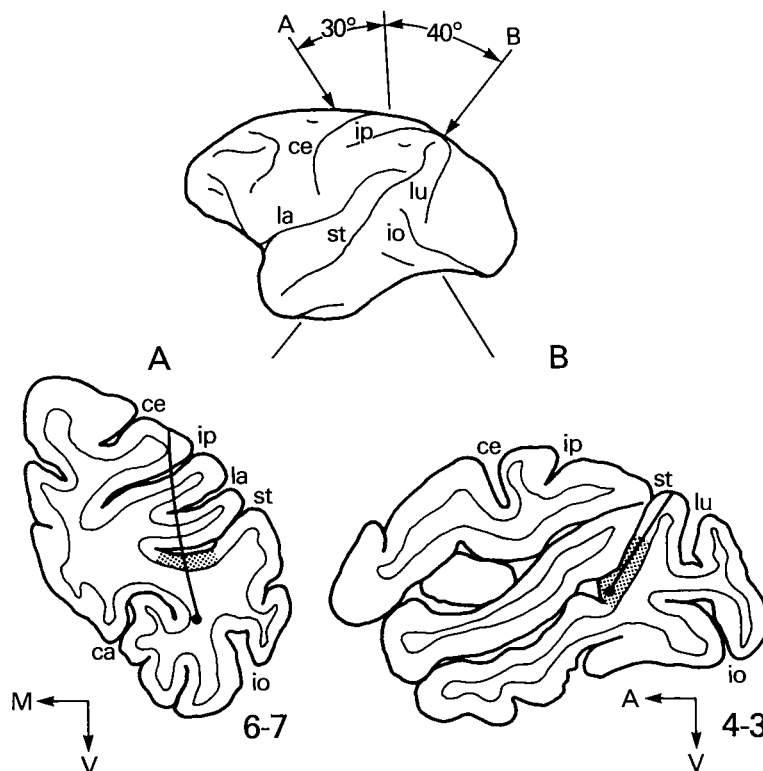


FIG. 1. Top: lateral view of the macaque brain showing penetration angles used to approach area MT. Angle A was used to obtain oblique and normal penetrations. A penetration made at this angle is shown in the section at lower left. Angle B was used to obtain tangential penetrations. A penetration made at this angle is shown in the parasagittal section at lower right. The stippled region in both sections indicates the location of area MT. ca, calcarine sulcus; ce, central sulcus; io, inferior occipital sulcus; ip, intraparietal sulcus; la, lateral sulcus; lu, lunate sulcus, st, superior temporal sulcus.

terminated every 100 μm in order to sample from a larger area of cortex. On rare occasions when a single cell could not be adequately isolated, the optimal direction preference of a small group of two or more cells was determined. Although the tuning range of these multiunits often tended to be broader, it was generally the case that when single cells in a group at a single recording site could be isolated, the optimal directions were similar (within a range of approximately 20°).

Visual stimuli

Visual stimuli were presented on a 60 x 60° rear-projection tangent screen with a background luminance of 2 cd/m^2 . Stimulus intensity was approximately 1.5 log units above background intensity. The optimal direction of motion was determined for each cell by use of a hand-held tungsten filament projector and an audio monitor of cellular activity. In some cases the accuracy of the subjective tuning estimate was verified with the use of a PDP-11/34A computer and an X-Y mirror optical system.

Stimuli consisted of moving white or colored spots subtending a minimal visual angle of 0.25° or elongated slits. Before the preferred direction of motion was assessed the optimal values of parameters such as stimulus size, color, contrast, and speed of motion were determined for each isolated unit. This optimal stimulus was then used in each eye separately to measure receptive-field size and to make the final assessment of preferred direction of motion and tuning range. For each cell an estimate was also made of the strength of response in the direction 180° from the optimal direction. Motion parallel to the horizontal meridian toward the ipsilateral visual field (leftward) was defined as 0° and direction of motion increased to 359° with counterclockwise rotations from this direction.

Histology

At the end of the 4-wk recording period, each animal was anesthetized with an overdose of sodium pentobarbital and perfused with saline followed by 10% buffered Formalin. The brain was then photographed and allowed to sink in sucrose Formalin.

In the three animals in which area MT was entered by electrode penetrations normal to the cortical surface, the brains were sectioned at 30° forward of the frontal plane. In the fourth animal the brain was sectioned in the parasagittal plane. Sections were cut at 33 μm and alternate sections were stained with cresyl violet and either a modified Heidenhain myelin stain (11) or a silver myelin stain (9). The position of area MT within the superior temporal sulcus was determined from the myeloarchitectonic boundaries seen in serial sections. The locations of all recording sites were determined on the bases of several small electrolytic lesions (4 μA, 20 s) made on each penetration. All electrode penetrations were reconstructed from serial sections and the laminar position of each recording site was established as well as its position relative to the myeloarchitectonic border of MT.

The angle of each penetration relative to the cortical surface was calculated from the penetration angles measured in both the plane of section and in the plane orthogonal to the plane of section. The angle of the penetration in the plane of section was measured relative to the radial fascicles of cells in the cortex. The angle of the penetration in the orthogonal plane was calculated by reconstructing the cortical surface from serial sections and estimating its slope. The angle of the penetration to the cortical surface is

$$\tan^{-1} (\tan^2 \theta + \tan^2 \phi)^{1/2}$$

where θ and ϕ are the penetration angles measured in the two orthogonal planes.

RESULTS

Five hundred sixty-two single units and 52 multiunits in area MT were studied on 21 penetrations in four *M. fascicularis*. The visual-field topography was found to conform to that previously reported (10, 29). Motion-sensitive units fell into four categories. The large majority (60%) of the cells were classified as directionally selective. These cells exhibited excitatory responses to stimulus motion in one direction but either did not respond to or were inhibited by motion in the opposite direction. A smaller proportion of cells (24%) were classified as directionally biased. These cells responded best to motion in one direction but also gave smaller excitatory responses to motion in the opposite direction. Another 8% of the sampled cells were bidirectional. These cells responded equally well to motion in two opposite directions. Finally, 8% of the cells were classified as pandirectional; that is, they responded equally well to motion in any direction. The distribution of preferred directions for all directionally selective and directionally biased cells is shown Fig. 2. Using a χ^2 test, we found that this distribution did not differ significantly from a uniform distribution, indicating that there were no significant tendencies to prefer motion in any particular direction ($\chi^2 = 12.88$, $df = 11$). Only 2% of

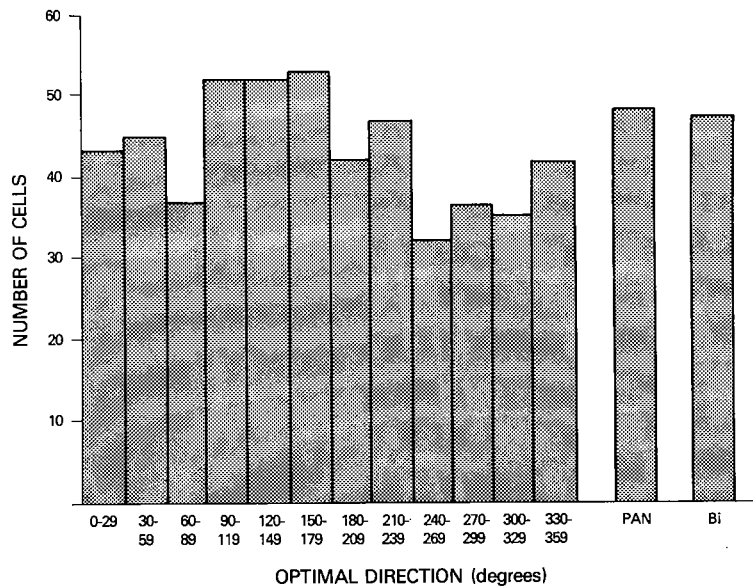


FIG. 2. Distribution of preferred directions of motion among unidirectional MT neurons and frequency of bidirectional (Bi) and pandirectional (PAN) neurons. Direction of motion varies counterclockwise from 0° (ipsilateral/leftward along the horizontal meridian).

our sampled cells showed obvious ocular dominance. Another 2% had opposite direction preferences when stimulated through each eye independently (also reported by Zeki (32)). Most MT neurons exhibited excitatory responses to the optimal stimulus anywhere within the receptive field.

The responses of most MT cells (55%) to a moving stimulus were independent of stimulus color, shape, or length, as previously reported by Zeki (31) and Maunsell and Van Essen (21). Of the remaining cells, 42% responded better to a small spot than to an elongated slit and 58% preferred an elongated slit over a small spot. For these cells, stimulus length affected the magnitude of response and the sharpness of directional tuning but not the preferred direction of motion. In a few cases, our qualitative estimate of preferred direction of motion was verified by computer and in no case was the difference greater than $\pm 10^\circ$.

The direction preference of each unit was determined using the optimal stimulus speed. Although we did not systematically study the effects of varying stimulus speed, direction preference was generally invariant across a broad range of speeds.

In a subsequent study (2) we found that many MT neurons also responded selectively to the orientation of a stationary slit, but the responses were invariably weaker than those to a moving stimulus.

Sequence regularity

On all penetrations into MT, direction preference tended to change systematically from one cell to the next over at least portions of the penetration, i.e., the representation of direction of motion exhibited "sequence regularity" (15). A penetration illustrating this property is shown in Fig. 3. This penetration entered MT at a fairly steep angle (approx-

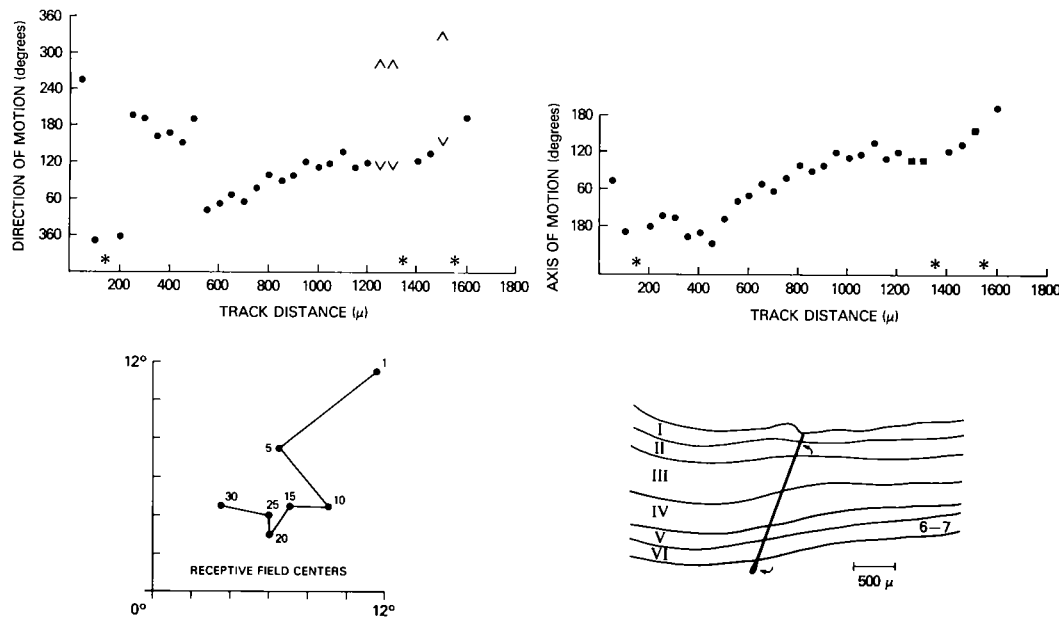


FIG. 3. Example of a penetration entering area MT at a steep angle to the cortical surface. Top left: optimal direction of stimulus motion as a function of electrode track distance. Each dot represents the optimal direction of motion for a single unidirectional cell. Opposing arrowheads represent the two direction preferences of a bidirectional cell. An asterisk along the abscissa represents a pandirectional cell. The progression of preferred directions is fairly regular with the exception of three large discontinuities near the beginning of the penetration. Top right: optimal axis of stimulus motion as a function of track distance. Squares represent the preferred axis of motion for bidirectional cells. The large discontinuities are eliminated, since they represent approximately 180° reversals. Plotting data in this manner emphasizes the continuity of the representation of axis of motion. Bottom left: receptive-field centers of representative cells along this penetration. Cell numbering corresponds with cells successively recorded at upper left and upper right. Bottom right: reconstruction of the electrode penetration in area MT. Recording sites are bounded by the two arrows.

mately 35° measured relative to the radial cell fascicles) within the representation of the central 10° of the visual field. Note that, with the exception of three large discontinuities near the beginning of the penetration, preferred direction of motion tended to shift gradually in a counterclockwise fashion. Thus, the cortex appeared to contain a systematic representation of direction of motion, although not necessarily a continuous one. The discontinuities in this and other penetrations were most often sudden shifts of approximately 180°. This observation suggested that the representation of optimal axis of motion might be more systematic than that of direction of motion, since opposite directions have a common axis of motion. Axis of motion may be defined as the orientation of the path along which a stimulus moves, independent of its direction along that path. Stimuli moving in opposite directions have a common axis of motion. Since the stimuli in this experiment were all moving on a tangent screen, axis is measured in this plane only and varies from 0 to 180°. When optimal axis of motion rather than direction of motion

is plotted as a function of track distance, the three large discontinuities in this penetration are eliminated, as shown at upper right, Fig. 3.

An example of sequence regularity along a more nearly tangential penetration is shown in Fig. 4. This penetration entered MT at 87° to the radial cell fascicles. Except for two discontinuities, preferred direction of motion tended to shift gradually along this penetration. Once again, the discontinuities, at 50 and 700 μm in this penetration, were approximately 180°. A plot of axis of motion versus track distance, shown in the upper right portion of Fig. 4, again indicates that the sequence regularity for axis of motion is, indeed, continuous.

In the previous two examples, the sequence regularity for direction of motion was clear in spite of the occasional discontinuity. In other penetrations, the sequence regularity of direction of motion was not so apparent due to the higher frequency of 180° reversals. A penetration of this type is shown in Fig. 5. This penetration entered MT at an acute angle (68°

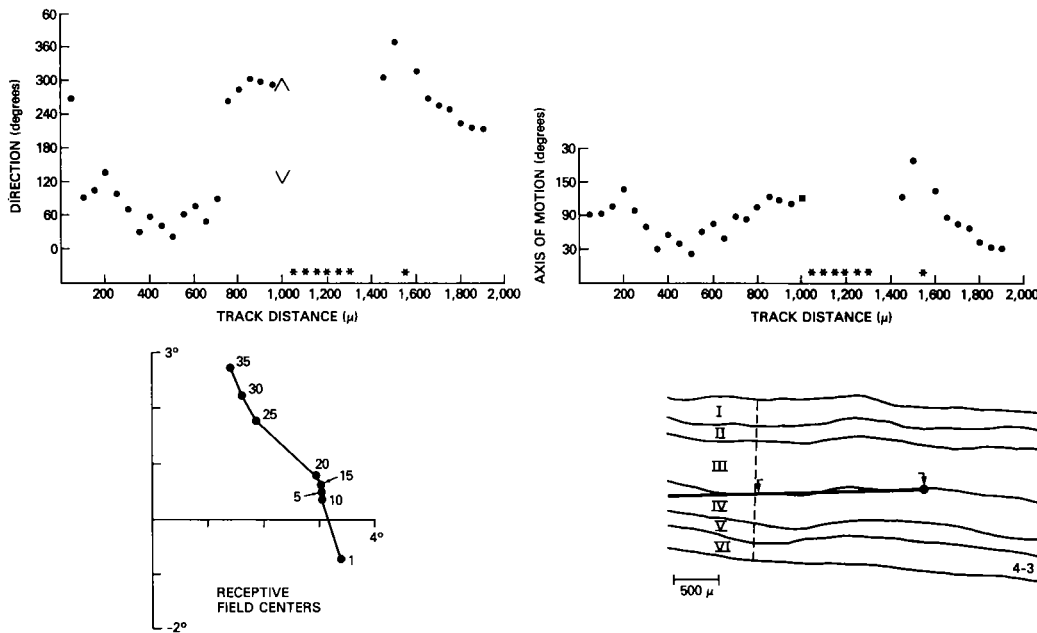


FIG. 4. Example of a penetration entering MT tangential to the cortical surface. Top left: optimal direction of stimulus motion as a function of electrode track distance. Top right: optimal axis of stimulus motion as a function of track distance. Bottom left: receptive-field centers of representative cells along this penetration. Bottom right: reconstruction of the electrode penetration in area MT. The dorsal myeloarchitectonic border of MT is indicated by the broken line across the cortex. See also legend to Fig. 3.

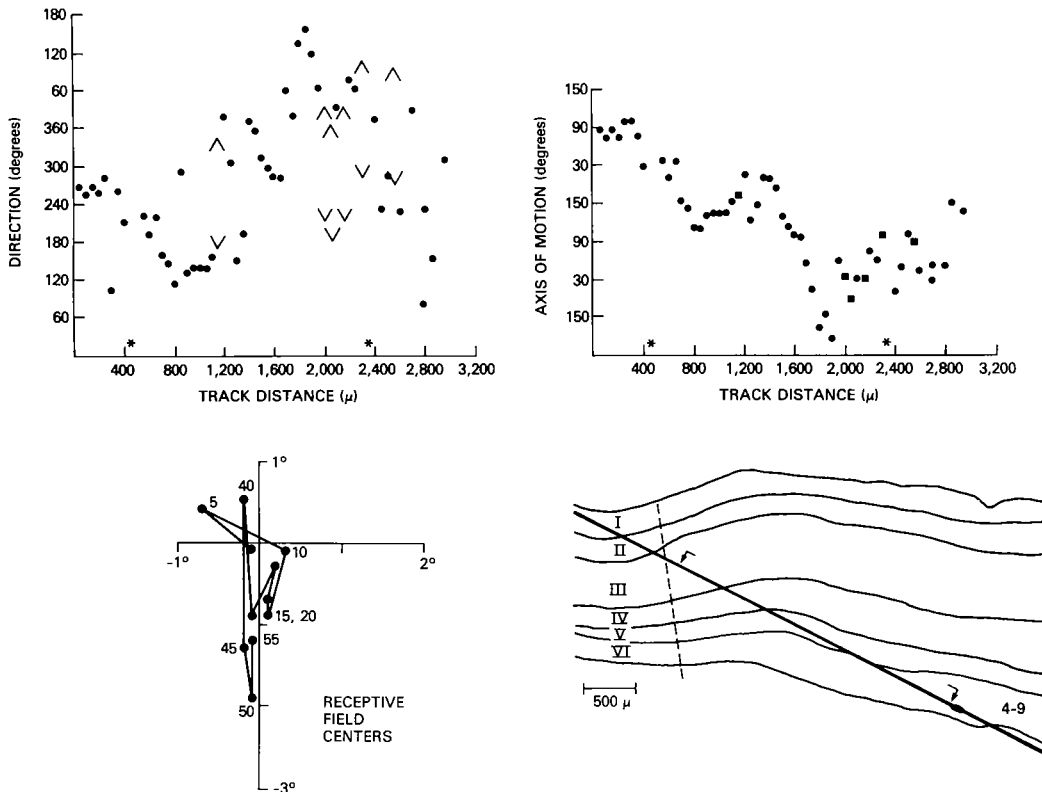


FIG. 5. Example of a penetration with a highly discontinuous progression of preferred directions of motion. Top left: optimal direction of stimulus motion as a function of track distance. This progression appears disorderly because of the large number of 180° reversals in preferred direction. Top right: optimal axis of stimulus motion as a function of track distance. As in the previous examples, the representation of axis of motion is more orderly. Bottom left: receptive-field centers of representative cells along this penetration. Bottom right: reconstruction of the electrode penetration in area MT. The dorsal myeloarchitectonic border of MT is indicated by the broken line across the cortex. See also legend to Fig. 3.

to the radial cell fascicles) within the parafoveal representation. Although there are small segments with an orderly progression of preferred direction, especially near the beginning of the penetration, the overall representation of direction appears chaotic. However, as in the previous examples, most of the discontinuities in the progression are approximately 180° . Thus, the plot of axis of motion at the upper right of Fig. 5 indicates a continuous representation, at least for the first two-thirds of the penetration.

Most of the penetrations, including those shown in Figs. 3–5, were confined to the representation of the central visual field in MT. A few penetrations, however, were made into the more peripheral field representation, and we saw the same systematic representation of direction and axis of motion as on the central

penetrations. An example is shown in Fig. 6. Along this penetration receptive-field centers were located in the lower contralateral visual field at eccentricities greater than 25° . The representation of direction of motion was at least as orderly on this peripheral penetration as on the more central ones. There was no systematic relationship between the eccentricity of any penetration and either the frequency of 180° reversals or the orderliness of the progression of preferred direction of motion.

The frequency distribution of angular change in preferred direction of motion between adjacent cells is shown in Fig. 7. The bimodal distribution reflects the tendency toward either small shifts or larger approximately 180° reversals in preferred direction of motion. (We found both of these peaks to

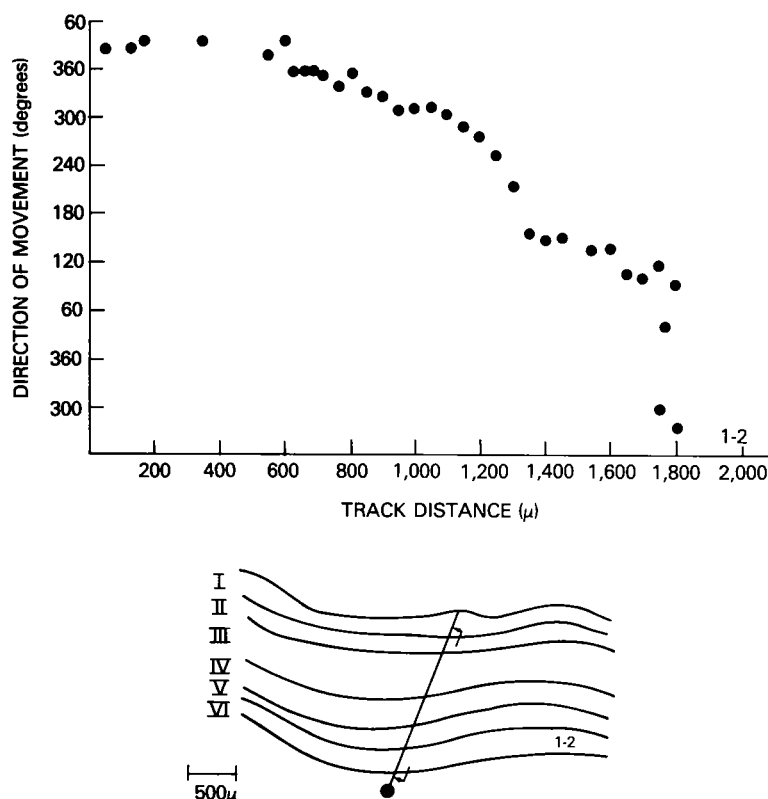


FIG. 6. Example of a penetration entering the peripheral visual field representation in MT. Receptive-field centers were greater than 25° eccentricity and located in the lower contralateral field. Top: optimal direction of stimulus motion as a function of electrode track distance. Bottom: reconstruction of this electrode penetration in area MT.

differ significantly from a uniform distribution (peak 1: $\chi^2 = 303.4$, $df = 1$, $P < 0.001$; peak 2: $\chi^2 = 9.0$, $df = 1$, $P < 0.01$.)

In summary, both preferred axis of motion and preferred direction of motion are represented in a regular, systematic fashion within MT. The representation of direction of motion appears regular but discontinuous, while the representation of axis of motion appears to be a more continuous one.

Columnar organization of axis of motion

The continuous shifts of preferred axis of motion observed as the penetrations traversed MT suggested that this area might contain radial or vertical columns of cells preferring the same axis of motion, analogous to orientation columns found within the striate cortex of the monkey, cat, and tree shrew (13, 15, 18). In the striate cortex, cells with the same orientation preference lie within the same vertical column (more accurately, the

same vertical "slab"), while preferred orientation shifts systematically from column to column. The most direct evidence for vertical axis of motion columns in MT would be vertical penetrations along which all cells have the same axis of motion preference. Unfortunately, due to the fact that MT is folded and buried within the STS, we were unable to make a penetration precisely normal to the surface of the cortex. The most nearly vertical penetration obtained was 13° from normal (Table 1). Since the distance moved parallel to the cortical surface is proportional to the sine of the angle of the penetration measured relative to the radial cell fascicles, this penetration covered $290 \mu\text{m}$ parallel to the surface over its 1.3 mm extent. Not surprisingly, preferred axis of motion did not remain constant over the entire extent of the penetration.

Although there is no direct evidence that cells within the same vertical column have the same axis of motion preference, it is possible

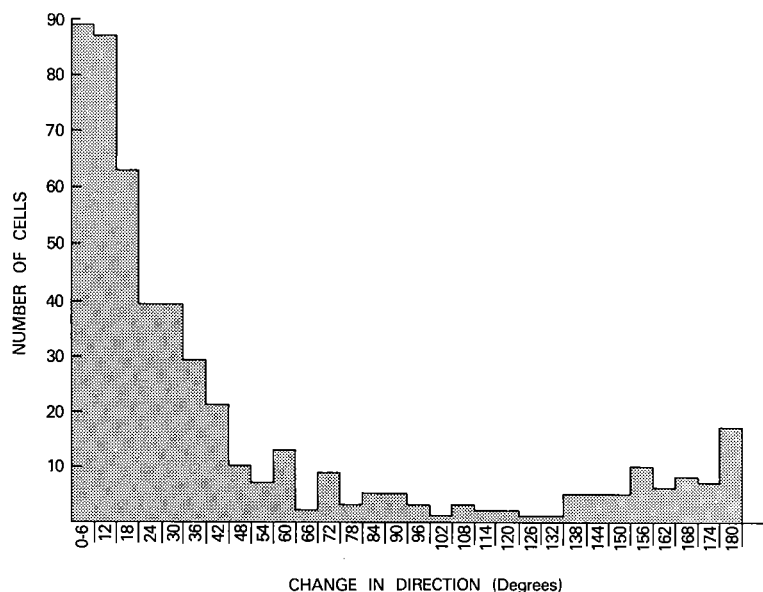


FIG. 7. Frequency distribution of changes in preferred direction of motion between adjacent unidirectional MT neurons (sampled at 50- μ m intervals). Peaks near 0 and 180° reflect the fact that adjacent neurons possess either very similar direction preferences or they differ by nearly 180°.

to reconstruct the representation of axis preference by estimating the rate of change of this parameter in different dimensions through the cortex. If a vertical or columnar type of organization for axis of motion exists, the maximal rate of change of preferred axis along a penetration should be proportional to the sine of the angle of the penetration, the most vertical penetrations having the smallest rate of change. This reflects the fact that on the average, the more tangential penetrations will intersect a greater number of columns than more normal penetrations.

In order to analyze the rate of change of axis of motion with respect to the angle of the penetrations, we first determined the rate of change of preferred axis for all sequences of cells on all penetrations, using the least-squares method of linear regression. We defined a sequence to be a segment of a penetration in which preferred axis of motion gradually rotated in only one direction (clockwise or counterclockwise). If the progression of preferred axis switched from clockwise to counterclockwise or vice versa, the sequence was ended and a new sequence started. Figure 8 illustrates how the regression lines were fitted for a typical penetration. Along the second

uninterrupted sequence in this penetration, the preferred axis of motion shifted in a clockwise direction. The rate of change was 168°/mm. The final two sequences had rates of change of 142 and 246°/mm, respectively.

We were able to fit regression lines in this manner to 84% of 36,500 linear micrometers of sampled cortex in area MT, corresponding to 42 sequences. For the remaining 16% of the sampled cortex we did not attempt to fit regression lines either because there were large gaps (at least 150 μ m) between successively recorded cells or because the number of successively recorded cells in a sequence was too small (fewer than 6) to provide a reliable estimate of rate of change of axis of motion.

Once a regression line was fitted to a sequence we calculated the standard error of residuals (SER) to be used as an index of "noise" in the representation of axis of motion. These SER values were roughly normally distributed with a mean of 15.5°/mm, a standard deviation of 9.0°/mm, and a range of 3.0–39.0°/mm. The SER values for the three sequences along the penetration shown in Fig. 8 were 24, 21, and 18°/mm, respectively. The SER values for all sequences to which a regression equation was fitted are listed in Ta-

TABLE 1. *Quantitative summary of results from oblique and tangential penetrations through area MT*

Penetration (Animal-Pass)	Sequence	Penetration Angle, deg	Mean Eccentricity, deg	Length of Sequence, μm		Rate of Change of Axis of Motion, deg/mm		SER	Layers
				Along track	Parallel to surface	Along track	Parallel to surface		
1-2	1	46	30	500	360	-12	-17	5	1-3
	2	46	30	1,200	864	-259	-360	23	3-6
1-4	1	18	17	600	186	78	252	10	1-3
1-6	1	13	8	300	66	10	45	4	2, 3
	3	13	8	350	77	-53	-241	3	4-6
1-7	1	25	11	700	294	142	338	19	1-3
	2	25	7	750	315	-107	-255	12	3-6
1-10	1	39	22	550	346	20	32	6	1-3
2-4	1	54	23	650	526	39	48	6	2, 3
	2	54	19	1,150	931	50	62	10	3-6
2-5	1	36	5	550	324	-177	-300	16	2-4
	2	36	3	700	413	179	303	20	4-6
2-8	1	37	13	600	360	-3	-5	12	2-6
2-10	1	29	35	1,150	552	8	17	26	1-6
4-3	2	87	3	300	297	-339	-342	16	3, 4
	3	87	3	500	495	175	177	12	4
	4	86	3	450	445	-313	-316	21	4, 5
4-4	1	83	3	500	495	74	75	11	3
	3	87	1	650	643	209	211	30	3
4-5	1	83	9	700	693	-35	-35	27	4
	2	86	6	900	891	-168	-170	24	4
	3	85	3	1,200	1,188	142	143	21	4
	4	81	2	1,100	1,089	-246	-248	18	3, 4
4-6	1	85	8	1,500	1,485	189	191	38	3, 4
	2	83	4	1,400	1,386	-18	-18	24	3
4-9	1	62	1	800	704	-200	-227	24	2-5
	2	66	1	550	500	115	126	18	5, 6
	3	71	1	300	285	-412	-435	10	6
	4	74	2	1,250	1,200	91	95	39	6
6-6	1	46	12	550	396	16	22	11	3
	2	46	11	350	252	-176	-244	4	3, 4
	3	46	7	450	324	320	444	14	4-6
6-7	1	35	9	1,500	855	129	226	21	2-6
6-8	1	39	20	450	283	4	6	4	1, 2
	2	39	16	500	315	294	467	12	3, 4
	3	39	9	450	283	-23	-36	7	4-6
6-9	1	22	8	1,600	592	107	289	19	2-6
6-11	1	22	17	850	314	-100	-270	10	3-5
	2	22	8	400	148	143	386	12	6
6-13	2	31	15	550	255	-15	-29	8	3-5
6-14	1	53	26	450	360	-210	-262	6	1-3
	2	53	21	650	520	96	120	17	3-5

ble 1. (The largest SER value was obtained from the final 1,250 μm of the penetration shown in Fig. 5.)

Noisy progressions, reflected by excessively large SER values, cannot be expected to provide accurate measures of rate of change of axis of motion. For this reason we rejected estimates of rate of change obtained from se-

quences with SER values greater than 1 SD above the mean, i.e., greater than $24.5^\circ/\text{mm}$. Five sequences failed to meet this criterion. Thus, 17% of the total length of sampled cortex that we were able to fit by linear regression (30,650 μm) contained a representation of axis of motion that was determined to be too noisy to provide an accurate measure of the rate of

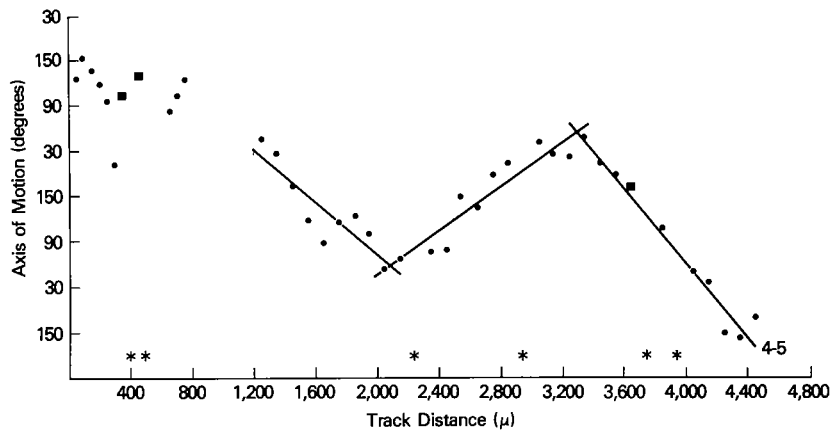


FIG. 8. Optimal axis of motion as a function of electrode track distance for a penetration through area MT. Cells were sampled at 100- μ m intervals along this penetration. Regression lines have been fitted to three continuous sequences in this penetration in order to obtain estimates of rate of change of axis of motion per millimeter of cortex along the electrode track. See Table 1 for actual rate-of-change values.

change of axis of motion. Table 1 provides the rate of change of axis of motion for all 42 sequences. These values range from a low of $3^\circ/\text{mm}$ to a high of $412^\circ/\text{mm}$.

We found that there was a proportional relationship between the sine of the penetration angle and the maximal rate of change of axis of motion. This relationship is shown in Fig. 9, where the rate of change of axis is plotted against the sine of the angle of the penetration, for all 37 sequences that met the criterion outlined above. The maximal rate of change increases as the penetrations range from 0° (or normal to the cortical surface) to 90° (or tangential to the surface). These data support the notion that cells within the same vertical column have the same preferred axis of motion. On the average, the rate of change of axis of motion is higher along tangential penetrations than along normal penetrations. However, there is considerable variation in the rate of change for penetrations at the same angle. This suggests that the axis of motion columns in MT, like the orientation columns in striate cortex, are more slablike than cylindrical. If the columns have an elongated or slablike shape, the rate of change of axis of motion would depend not only on the angle of the penetration to the cortical surface but also on the angle at which the penetration intersected the slabs. The upper limit on the rate of change is determined by the angle to the surface, but a penetration may have a lower rate of change

if it moves parallel to the slabs (see diagram, Fig. 9, upper left).

Column size

If the axis of motion slabs are uniform in size and shape, the highest rates of change of preferred axis of motion will be on penetrations that cut across the axis of motion slabs orthogonally. Therefore, the minimum size of the complete representation of 180° of axis of motion can be estimated from the sequences that have the highest rates of change. When the length of each sequence is adjusted to reflect the distance traveled parallel to the cortical surface (by dividing by the sine of the penetration angle; see Table 1), the highest rates of change appear to cluster around $420^\circ/\text{mm}$. This rate can also be derived from the data in Fig. 9, where only three sequences have a rate greater than $420^\circ/\text{mm}$ times the sine of the penetration angle. Thus, if we accept $420^\circ/\text{mm}$ as a reasonable limit on the maximum rate of change, then a full 180° of axis of motion is contained within approximately 400–500 μm of the cortex.

Direction of motion versus axis of motion

We have stressed the columnar organization of axis of motion in MT, since the representation of axis of motion appears to be more continuous than the representation of direction of motion. Does direction of motion preference alternate (randomly or systemati-

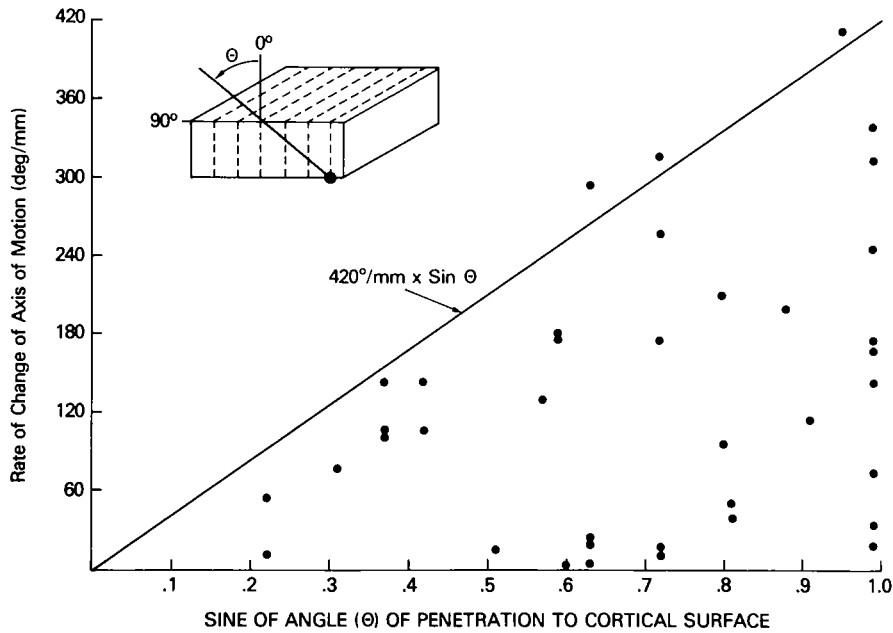


FIG. 9. Observed rate of change of optimal axis of motion as a function of the sine of the electrode angle relative to the radial cell fascicles. Each point represents rate of change measured along the length of the electrode track for a single sequence of constant rate. Electrode angle 0° represents a penetration normal to the cortical surface and an angle of 90° represents a tangential penetration. On the average, rate of change is higher along tangential penetrations than along normal penetrations, supporting the notion that cells within the same vertical column have the same preferred axis of motion. The variation in rate of change for penetrations of the same angle suggests that axis of motion columns are more slablike than cylindrical. If columns are elongated, the rate of change of axis of motion will depend not only on the angle of the penetration to the cortical surface but also on the angle of the penetration relative to the elongated slabs. The maximal value, however, will be determined solely by the angle of the penetration to the cortical surface and will vary proportionally with the sine of this angle. A rough estimate of the maximal rate of change for any penetration angle was therefore obtained by fitting the solid line that falls very near the maximal observed values. Thus, on a tangential penetration, the predicted maximal rate of change of axis of motion is $420^\circ/\text{mm}$, or roughly $180^\circ/430 \mu\text{m}$.

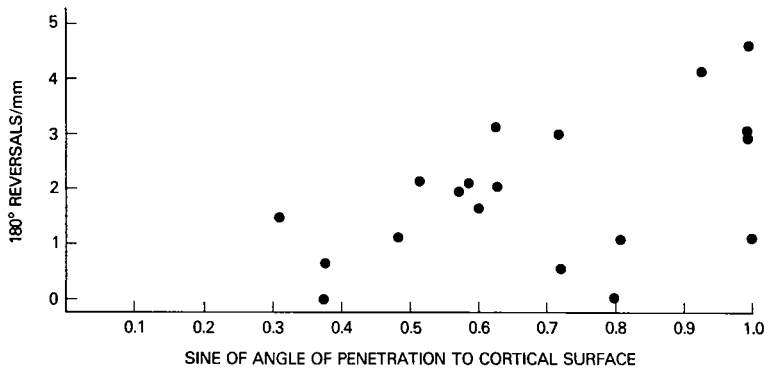


FIG. 10. Observed frequency of 180° reversals in optimal direction of motion between adjacent MT neurons as a function of the sine of the electrode angle relative to the radial cell fascicles. Each point represents the frequency of reversals (reversals per millimeter) measured along the length of the electrode track for each penetration. Electrode angle 0° represents a penetration normal to the cortical surface. On the average, reversals are more frequent along tangential penetrations, suggesting that cells with opposite direction of motion preferences lie in adjacent vertical columns rather than within the same vertical column of cells.

cally) between cells within a vertical axis of motion column, or do they lie in separate (but adjacent) vertical direction of motion columns? If direction of motion reverses within vertical columns, the frequency of 180° reversals should be highest on the most normal penetrations. If, however, direction of motion preference alternates horizontally between adjacent cells within the cortex, the most tangential penetrations should have the highest frequencies of reversals. In Fig. 10, the frequency of 180° ($\pm 25^\circ$) reversals is plotted against the sine of the penetration angles. On the average, reversals are more frequent on the more tangential penetrations, (the slope of the regression line fitted to the points in Fig. 10 is significantly greater than zero; Student's t , $P < 0.05$) suggesting that direction of motion alternates or reverses within the horizontal dimension of the cortex in MT and that cells with the same direction preference lie within the same vertical column. Thus, within a single axis of motion slab there may be at least two direction of motion columns with opposite direction preferences.

DISCUSSION

The present results confirm previous reports that most MT neurons are sensitive to the direction of stimulus motion. We have also confirmed the observation that nearby cells in area MT tend to have similar direction preferences. Moreover, we have now demonstrated that this tendency reflects a columnar organization for directionally selective cells within MT. Cells sensitive to the same axis of motion are organized in vertical slabs, and within single axis slabs, cells sensitive to opposite directions of motion also appear to be arranged in separate columns. This is the first physiological demonstration of a columnar architecture in a monkey extrastriate visual area and it is supported by the recent demonstration by Burkhalter et al. (7) of a columnar pattern of 2-deoxyglucose labeling in MT following unidirectional stimulation. These results suggest that the analysis of visual motion is a fundamental property of area MT. Furthermore, they lend additional weight to the theory that the basic unit of cortical organization is the column or "module."

The remainder of the discussion will consider 1) the similarity between axis of motion

columns in MT and orientation columns in striate cortex, 2) the relationship between axis of motion columns and direction columns, 3) the structure and precision of the columnar arrangement in MT, and 4) the relevance of functional architecture in MT to its role in vision.

Comparison with striate cortex

The similarities between the representation of axis of motion in MT and orientation specificity in striate cortex are striking. In each cortical area, the representation is constant within a vertical column but varies nearly continuously across columns, with occasional breaks and reversals (but cf. Ref. 5). The size of the columnar systems is also comparable in the two areas, about 0.5 mm both for 180° of orientation in striate cortex (15) and for 180° of axis of motion representation in MT.

There is an additional similarity between MT and striate cortex. Recent reports indicate that in the cat, cells in striate cortex with the same direction of motion preference are located within the same vertical column and that separate columns with opposite direction preference are located within the same orientation slab (23, 27). In area MT, direction of motion columns appear to have a similar relationship to axis of motion slabs.

The major difference between the columnar systems in MT and striate cortex is the difference between axis of motion selectivity and orientation selectivity. While most cells in striate cortex are more sensitive to the orientation of a moving or stationary stimulus than to its direction of motion, the reverse is true in MT. Moreover, unlike most cells in striate cortex, most MT cells respond nearly as well to a small spot (i.e., small relative to receptive-field size) or a field of random visual noise moving in the optimal direction as to a moving slit. Furthermore, the orientation preference of some MT neurons, measured with stationary flashed stimuli, does not coincide with the axis of motion preference (2, 21). Indeed, in some cases orientation preference is parallel to the preferred axis of motion. Thus, orientation and axis of motion preference cannot be used interchangeably for MT neurons as they can for neurons in striate cortex. While stimulus orientation appears to be a more relevant stimulus dimension in striate cortex, the axis of stimulus motion ap-

pears to be a more relevant dimension in MT. Consequently, we refer to the columnar system in MT as composed of axis of motion columns rather than orientation columns.

Geometry of columnar system

Our data are insufficient to reveal the overall geometry of the axis of motion columns. Since the representation of axis of motion is highly regular, it is likely to exist in the form of continuous slabs. Any of the models that have been proposed for the arrangement of orientation columns in striate cortex, such as parallel or radial slabs (6, 15, 25), may apply to MT as well. (Indeed, the arrangement of orientation columns in striate cortex is still unclear (5, 12).) In contrast to axis of motion, the global representation of direction of motion is not restricted to continuous slabs, since it is periodically interrupted by 180° reversals. Columns of directionally selective cells could exist as discrete islands and could be arranged either regularly or randomly within a single axis of motion slab. Since there were many penetrations in MT with infrequent direction of motion reversals over long distances, the columns with opposite direction preferences, although adjacent (to explain abrupt reversals), must each be fairly wide. It is tempting to speculate that there may be alternating rows of direction columns in MT. Within a row, direction may be represented continuously from 0 to 360° . Across rows, direction may "flip" 180° from one row to the next (see Fig. 11).

Column structure

Hubel and Wiesel (15) have argued that in electrode penetrations through macaque striate cortex they can detect discrete steplike changes in orientation preference as the electrode is advanced parallel to the cortical surface, suggesting that the orientation columns are discrete entities (with little or no variability in orientation within each). Alternatively, Albus (3) claims that the distribution of orientation-selective cells within an orientation column in cat striate cortex is roughly Gaussian. That is, on moving from one column to the next, one continues to find cells with the same preference but with reduced frequency. Thus, the columns are more statistical than discrete entities.

In our study of columnar structure in area MT we were unable to detect discrete, uniform

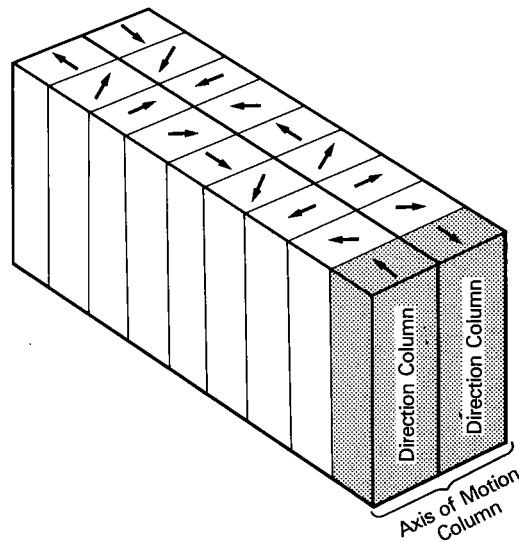


FIG. 11. Three-dimensional depiction of a block of cortical tissue containing one configuration of axis and direction of motion columns that is consistent with our data. The vertical dimension represents cortical depth. The long axis of the figure may be viewed as two complete revolutions of axis of motion columns. Moving in this dimension, one would encounter gradual changes in preferred direction. Within each axis of motion column (along the short axis of the figure) the two opposite directions of motion along that axis of motion are represented as adjacent columns. Moving in this dimension, one would encounter frequent 180° reversals in preferred direction, with no change in preferred axis of motion.

changes in axis or direction of motion preference in tangential penetrations. Thus, it seems likely that direction is represented in a continuous (possibly Gaussian) fashion across the cortex of MT rather than in the form of discrete columns.

Representation of direction of motion—precision

On most of our penetrations through MT, preferred axis or direction of motion changed smoothly from one cell to the next. However, on some sequences, there was a considerable degree of noise or "scatter" about the general trend. An example of such a sequence is provided by the last $1,250 \mu\text{m}$ along the penetration shown in Fig. 5, which has a large amount of scatter about a general counterclockwise progression. Moreover, for a number of sequences the standard error of the residuals about the fitted regression lines was excessively large. Thus, on some penetrations,

sequence regularity of axis of motion appears poor when contrasted with the high degree of orientation sequence regularity seen in published data from the striate cortex of macaques (15), tree shrews (18), and cats (3, 13, 19).

This noise in the representation of axis of motion may be in part attributable to the difficulty in obtaining a precise estimate of preferred direction of motion for many cells. The precision of such a measure is inversely proportional to the tuning bandwidth of a cell. Many MT cells are broadly tuned to direction of motion. The mean direction-tuning bandwidth (full width, half maximum) for a moving slit in area MT is 91° (2), roughly 1.5 times the orientation bandwidth of cells in striate cortex (8, 24; T. D. Albright, unpublished observations). In some cases the preferred direction of a cell can only be estimated to $20\text{--}30^\circ$, which is about the scatter in preferred direction for the noisier sequences. In other sequences, however, uncertainty in estimating preferred direction cannot account for all of the scatter. In some cases, preferred direction jumps nearly 90° from cell to cell, almost certainly reflecting discontinuities in the local columnar organization. Interestingly, a parallel situation exists in the visuotopic organization of MT. Overall, MT is topographically organized but there is substantial scatter in the receptive-field location from one cell to the next (10, 29). We have tried to correlate the scatter in direction preference in our penetrations with scatter in receptive-field trajectories. Although there are several sequences exhibiting disorganized direction progressions and also particularly tortuous receptive-field trajectories (e.g., see Fig. 5), we were unable to find a consistent relationship between direction-sequence regularity and receptive-field scatter. Furthermore, we found no relationship

between either sequence regularity or receptive-field scatter and cortical layer. (In striate cortex, Bauer et al. (5) recently reported an orientation shift between the supragranular and infragranular layers.)

Role of MT in vision

The present findings demonstrate that cells with similar preferred axes of motion and cells with similar preferred directions of motion are organized into vertical columns and suggest that area MT plays a fundamental role in the analysis of stimulus motion. In macaque striate cortex, approximately $500\ \mu\text{m}$ of the cortex includes cells with receptive fields representing the same portion of the visual field and these cells include a full complement of preferred orientations (15–17). Although MT is much smaller than striate cortex, because of its larger receptive fields approximately $500\ \mu\text{m}$ of MT also includes cells with receptive fields that overlap in the visual field. This area includes cells representing a full complement of direction of motion preferences. Thus, in both MT and striate cortex, a roughly $500\text{--}\mu\text{m}$ -wide region of cortex contains the neural machinery sufficient to process information about a specific stimulus parameter in one portion of the visual field.

ACKNOWLEDGMENTS

We thank T. Farris and S. Gorlick for assistance with histology and data analysis; C. Colby, S. Fenstemaker, R. Gattass, I. Jeffers, M. Mishkin, J. Moran, C. Olson, and H. Rodman for their comments on the manuscript; and S. Rodgers for typing.

This study was supported by National Institutes of Health Grant MH-19420 and National Science Foundation Grant BNS-8200806.

Received 6 January 1983; accepted in final form 25 July 1983.

REFERENCES

- ALBRIGHT, T. D., DESIMONE, R., AND GROSS, C. G. Organization of directionally selective cells in area MT of macaques. *Soc. Neurosci. Abstr.* 7: 832, 1981.
- ALBRIGHT, T. D. AND GROSS, C. G. Direction and orientation selectivity of neurons in area MT of macaques. *Soc. Neurosci. Abstr.* 8: 811, 1982.
- ALBUS, K. A quantitative study of the projection area of the central and paracentral visual field in area 17 of the cat. II. The spatial organization of the orientation domain. *Exp. Brain Res.* 24: 181–202, 1975.
- BAKER, J. F., PETERSON, S. E., NEWSOME, W. T., AND ALLMAN, J. M. Visual response properties of neurons in four extrastriate visual areas of the owl monkey (*Aotus trivirgatus*): a quantitative comparison of medial, dorsomedial, dorsolateral, and middle temporal areas. *J. Neurophysiol.* 45: 397–416, 1981.
- BAUER, R., DOW, B. M., SNYDER, A. Z., AND VAUTIN, R. Orientation shift between upper and lower layers in monkey visual cortex. *Exp. Brain Res.* 50: 133–145, 1983.
- BRAITENBERG, V. AND BRAITENBERG, C. Geometry of orientation columns in the visual cortex. *Biol. Cybern.* 33: 179–186, 1979.
- BURKHALTER, A., VAN ESSEN, D. C., AND MAUNSEEL, J. H. R. Patterns of 2-deoxyglucose labeling in extrastriate visual cortex of unstimulated and uni-

- directionally stimulated macaque monkeys. *Soc. Neurosci. Abstr.* 7: 172, 1981.
8. DEVALOIS, R. L., YUND, E. W., AND HELPER, N. The orientation and direction selectivity of cells in macaque visual cortex. *Vision Res.* 22: 531-544, 1982.
 9. GALLYAS, F. Silver staining of myelin by means of physical development. *Orvostudomány* 20: 433-489, 1969.
 10. GATTASS, R. AND GROSS, C. G. Visual topography of striate projection zone in posterior superior temporal sulcus (MT) of the macaque. *J. Neurophysiol.* 46: 621-638, 1981.
 11. GATTASS, R., GROSS, C. G., AND SANDELL, J. H. Visual topography of V2 in the macaque. *J. Comp. Neurol.* 201: 519-539, 1981.
 12. HUBEL, D. H. AND LIVINGSTONE, M. S. Regions of poor orientation tuning coincide with patches of cytochrome oxidase staining in monkey striate cortex. *Soc. Neurosci. Abstr.* 7: 357, 1981.
 13. HUBEL, D. H. AND WIESEL, T. N. Shape and arrangement of columns in cat's striate cortex. *J. Physiol. London* 165: 559-568, 1963.
 14. HUBEL, D. H. AND WIESEL, T. N. Receptive fields and functional architecture of monkey striate cortex. *J. Physiol. London* 195: 215-243, 1968.
 15. HUBEL, D. H. AND WIESEL, T. N. Sequence regularity and geometry of orientation columns in the monkey striate cortex. *J. Comp. Neurol.* 158: 267-294, 1974.
 16. HUBEL, D. H. AND WIESEL, T. N. Uniformity of monkey striate cortex: a parallel relationship between field size, scatter and magnification factor. *J. Comp. Neurol.* 158: 295-306, 1974.
 17. HUBEL, D. H., WIESEL, T. N., AND STRYKER, M. P. Anatomical demonstration of orientation columns in macaque monkey. *J. Comp. Neurol.* 177: 361-379, 1978.
 18. HUMPHREY, A. L. AND NORTON, T. T. Topographic organization of the orientation column system in the striate cortex of the tree shrew (*Tupaia glis*). I. Microelectrode recording. *J. Comp. Neurol.* 192: 531-547, 1980.
 19. LEE, B. B., ALBUS, K., HEGGELUND, P., HULUME, M. J., AND CREUTZFELDT, O. D. The depth distribution of optimal stimulus orientations for neurons in cat area 17. *Exp. Brain Res.* 27: 301-313, 1977.
 20. LEVAY, S., HUBEL, D. H., AND WIESEL, T. N. The pattern of ocular dominance columns in macaque visual cortex revealed by a reduced silver stain. *J. Comp. Neurol.* 159: 559-576, 1975.
 21. MAUNSELL, J. H. R. AND VAN ESSEN, D. C. Functional properties of neurons in middle temporal visual area of the macaque monkey. I. Selectivity for stimulus direction, spread and orientation. *J. Neurophysiol.* 49: 1148-1167, 1983.
 22. MICHAEL, C. R. Columnar organization of color cells in monkey's striate cortex. *J. Neurophysiol.* 46: 587-604, 1981.
 23. PAYNE, B. R., BERMAN, N., AND MURPHY, E. H. Organization of direction preferences in cat visual cortex. *Brain Res.* 211: 445-450, 1980.
 24. SCHILLER, P. H., FINLAY, B. L., AND VOLMAN, S. F. Quantitative studies of single cell properties of monkey striate cortex. II. Orientation specificity and ocular dominance. *J. Neurophysiol.* 39: 1320, 1976.
 25. SCHWARTZ, E. L. Computational anatomy and functional architecture of striate cortex: a spatial mapping approach to perceptual coding. *Vision Res.* 20: 645-669, 1980.
 26. SILVERMAN, M. S., TOOTELL, R. B. M., AND DEVALOIS, R. L. Deoxyglucose mapping of orientation and spatial frequency in cat visual cortex. *Invest. Ophthalmol. Suppl.* 19: 225, 1980.
 27. TOLHURST, D. J., DEAN, A. F., AND THOMPSON, I. D. Preferred direction of movement as an element in the organization of cat visual cortex. *Exp. Brain Res.* 44: 340-342, 1981.
 28. UNGERLEIDER, L. AND MISHKIN, M. The striate projection zone in the superior temporal sulcus of *Macaca mulatta*: location and topographic organization. *J. Comp. Neurol.* 188: 347-366, 1979.
 29. VAN ESSEN, D. C., MAUNSELL, J. H. R., AND BIXBY, J. L. The middle temporal visual area in the macaque: myeloarchitecture, connections, functional properties and topographic connections. *J. Comp. Neurol.* 199: 293-326, 1981.
 30. VAN ESSEN, D. C. AND ZEKI, S. M. The topographic organization of rhesus monkey prestriate cortex. *J. Physiol. London* 277: 193-226, 1978.
 31. ZEKI, S. M. Functional organization of a visual area in the posterior bank of the superior temporal sulcus of the rhesus monkey. *J. Physiol. London* 236: 549-573, 1974.
 32. ZEKI, S. M. Cells responding to changing image size and disparity in the cortex of the rhesus monkey. *J. Physiol. London* 242: 827-841, 1974.
 33. ZEKI, S. M. Uniformity and diversity of structure and function in rhesus monkey prestriate cortex. *J. Physiol. London* 277: 272-290, 1978.
 34. ZEKI, S. M. Functional specialization in the visual cortex of rhesus monkey. *Nature London* 274: 245-272, 1978.